Low-speed Modeling and Simulation of Torpedo-shaped AUVs

Bjarni Helgason[1], Leifur Leifsson[1], Indridi Rikhardsson[1], Helgi Thorgilsson[2] and Slawomir Koziel[3]
[1]*CADIA/Laboratory for Unmanned Vehicles, School of Science and Engineering, Reykjavik University, Reykjavik, Iceland*
[2]*Teledyne Gavia ehf, Vesturvor 29, 200 Kopavogur, Iceland*
[3]*Engineering Optimization & Modeling Center, School of Science and Eng., Reykjavik University, Reykjavik, Iceland*

Keywords: Autonomous Underwater Vehicle, Low-speed Motion, Vehicle Dynamics, Simulation, Experimental Validation.

Abstract: Autonomous underwater vehicles (AUVs) have become important in many marine engineering applications, such as environmental monitoring, pipeline inspections, or oceanography. For these types of applications, most of the AUVs available in both academia and industry are shaped like a torpedo and travel at speeds of 3 knots or higher. There is an growing interest in AUVs that are capable of performing tasks at both low-speed as well as high speeds. Currently, many torpedo-shaped AUVs are not capable of controlled low-speed motion. This paper presents a simulation model for the low-speed motion of torpedo-shaped AUVs. The model is capable of simulating the surge, sway, heave, and yaw motions. The hydrodynamic forces acting on the AUV hull are modelled using strip theory, experimental data, and computational fluid dynamics. The simulation model was implemented using a commercially available software and validated using experimental data obtained from the Gavia AUV. The results show that the simulation model captures the AUV motion at low-speed and agrees well with the experimental data.

1 INTRODUCTION

An autonomous underwater vehicle (AUV) is a robot which travels underwater without requiring any input from an operator (Fossen, 1994). The tasks and missions of AUVs are constantly evolving and becoming increasingly important for commercial-, military-, research- and hobby users. A typical commercial job for an AUV is, e.g., to construct detailed maps of the seafloor before building subsea infrastructure in the oil and gas industry. A typical military mission for an AUV is to map an area and determine if there are any mines, or to monitor a protected area for unidentified objects. Scientists use AUVs to study lakes, the ocean and the ocean floor.

Numerous AUVs have been developed, both in academia, e.g., (Clark et al., 2009; Ananthakrishnan and Decron, 2000; de Barros et al., 2008; Kennedy, 2002), and in the industry, e.g., (Allen et al., 2000). These vehicles are of various shapes and sizes. AUV's intended for high-speed (higher than 3 knots) and long-range (longer than 6 hours) missions are commonly torpedo-shaped with aft-mounted propulsion and control systems (Braunl et al., 2007; Eastman et al., 2009). AUVs designed for performing tasks at low speeds differ, but (usually) their shapes are not streamlined, as it is not necessary. However, they are (normally) equipped with several thrusters for manoeuvring in all directions. There is an growing interest in AUVs that are capable to perform tasks at both low- (or zero) and high-speeds (Braunl et al., 2007). Currently, many torpedo-shaped AUVs are not capable of controlled low-speed motion.

The objective of this research is to investigate the low-speed characteristics of torpedo shaped AUVs and their control. In particular, we model the vehicle motion at low-speed and develop a computational framework capable of simulating the vehicle response. We use the commercially available Gavia AUV[1] as a testbed (Fig. 1). The model is validated and tuned using data from physical experiments.

Figure 1: The Gavia AUV is commercially available and is capable of various missions, such as oceanography and pipeline inspection.

[1]www.gavia.is

Helgason B., Leifsson L., Rikhardsson I., Thorgilsson H. and Koziel S..
Low-speed Modeling and Simulation of Torpedo-shaped AUVs.
DOI: 10.5220/0004047103330338
In *Proceedings of the 9th International Conference on Informatics in Control, Automation and Robotics* (ICINCO-2012), pages 333-338
ISBN: 978-989-8565-22-8

2 GOVERNING EQUATIONS FOR LOW-SPEED MOTION

We want to move the AUV in certain directions during low-speed motion. In particular, we want to move the AUV back and forth, up and down, to the sides, and rotate it. Therefore, only four degrees of freedom are required. In this section, we describe the governing equations for such motion and we develop specific models for the system dynamics.

2.1 General Equations and Frames of Reference

Two coordinate frames must be defined to describe the motion of underwater vehicles (Fig. 2). The moving coordinate frame $X_0Y_0Z_0$ is fixed to the vehicle and is called the body-fixed reference frame and the fixed coordinate frame XYZ is the earth coordinate system (Fossen, 1994). The fixed coordinate system is an earth coordinate system while the moving one follows vehicle heading and location each time. The $X-$axis is in line with length of vehicle and center of gravity, where positive movement means forward and vice versa. All movement in line with the $X-$axis is surge (u is surge velocity) movement, while rotation about the axis is roll (p) rotation. Axes Y and Z then follow the $X-$axis as in a regular coordinate system. Movement in line with Y-axis is sway (v is sway velocity), while rotation about same axis is pitch (q) rotation. Movement in line with Z-axis is heave (w is heave velocity), while rotating about same axis is yaw (r) rotation.

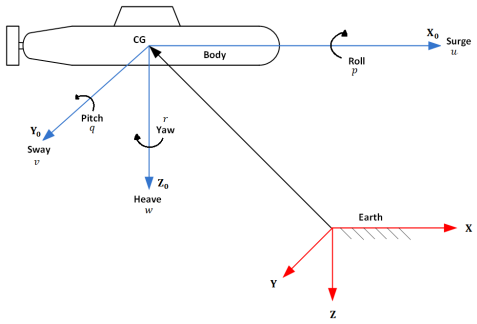

Figure 2: Coordinate systems, both body-fixed and earth-fixed.

At low speed, the AUV moves in one direction at a time. In particular, the AUV moves along the axes of surge, sway and heave, and rotates (yaws) about heave axis. The general governing equations of motion along each of these axes are (Fossen, 1994)

$$m\left[\dot{u}-vr+wq-x_G(q^2+r^2)+y_G(pq-\dot{r})+z_G(pr+\dot{q})\right]=\sum X_{ext} \quad (1)$$

$$m\left[\dot{v}-wp+ur-y_G(r^2+p^2)+z_G(qr-\dot{p})+x_G(qp+\dot{r})\right]=\sum Y_{ext} \quad (2)$$

$$m\left[\dot{w}-uq+vp-z_G(p^2+q^2)+x_G(rp-\dot{q})+y_G(rq+\dot{p})\right]=\sum Z_{ext} \quad (3)$$

$$I_z\dot{r}+(I_y-I_x)pq+m\left[x_g(\dot{v}-wp+ur)-y_G(\dot{u}-vr+wg)\right]=\sum N_{ext} \quad (4)$$

where m is the rigid body mass, I is the rigid body inertia about a specific axis, x_G, y_G and z_G are each axis distance from the rigid body center of gravity, X_{ext}, Y_{ext}, Z_{ext} are forces acting of the vehicle in their respective axes, and N_{ext} is the moment about the Z_0-axis.

We will now analyze each of these equations for the low-speed motion of torpedo-shaped AUVs.

2.2 Surge Motion

The external forces acting on the AUV in the surge direction are due to the thrust, drag and added mass. The governing surge equation of motion, Eq. (1), becomes, when taking into account these external forces, as well as neglecting motion in other directions,

$$m\dot{u}=-X_{\dot{u}}\dot{u}-D_{surge}u+T_{surge}, \quad (5)$$

where $X_{\dot{u}}$ is the added mass derivative for surge, D_{surge} is the hydrodynamic drag for surge, and T_{surge} is the surge thrust force. Effects due to Coriolis and centripetal forces are neglected.

In this work, we estimate the added mass derivatives using strip theory for slender bodies (Fossen, 1994). The added mass derivative for surge is (Helgason, 2012)

$$X_{\dot{u}}\simeq -0.1m. \quad (6)$$

The hydrodynamic drag is modelled as (Wang and Clark, 2007)

$$D=D_L+D_Q, \quad (7)$$

where D_L and D_Q are the linear and quadratic drag terms, respectively. The linear term is determined by experiments, and the quadratic term is

$$D_Q=C_{D_{surge}}\frac{1}{2}\rho A_{surge}u|u|, \quad (8)$$

where $C_{D_{surge}}$ is the drag coefficient for surge motion, ρ is the water density, A_{surge} is the reference area for surge motion. The surge drag coefficient is determined using computational fluid dynamics (CFD) and the resulting value is $C_{D_{surge}} = 0.37$ (Helgason, 2012).

2.3 Sway Motion

Same type of forces act on the AUV in the sway direction as in the surge one. The governing sway equation of motion, Eq. (2), becomes (Helgason, 2012)

$$m\dot{v} = -Y_{\dot{v}}\dot{v} - D_{sway}v + T_{sway}, \quad (9)$$

where $Y_{\dot{v}}$ is the added mass derivative for sway, D_{sway} is the hydrodynamic drag for sway, and T_{sway} is the sway thrust force. Strip theory yields the added mass derivative as (Helgason, 2012)

$$Y_{\dot{v}} \simeq -\pi\rho R^2 L, \quad (10)$$

where R is the maximum radius of the AUV hull and L is it's length. The drag is modelled in the same way as for the surge motion, i.e., Eqs. (7) and (8). However, the quadratic drag coefficient in the sway direction is estimated based on experimental data for circular cylinder in cross-flow and is taken to be $C_{D_{sway}} = 1.2$ (White, 2008).

2.4 Heave Motion

In the heave direction, the same external forces act on the vehicle as in the surge and sway directions, including the gravitational and buoyancy forces. The governing heave equation of motion, Eq. (3), is then (Helgason, 2012)

$$m\dot{w} = -Z_{\dot{w}}\dot{w} - D_{heave}w - (f_g + f_b) + T_{heave}, \quad (11)$$

where $Z_{\dot{w}}$ is the added mass derivative for heave, D_{heave} is the hydrodynamic drag for heave, f_g is the vehicle weight, f_b is the vehicle buoyancy force, and T_{heave} is the heave thrust force. The added mass derivative term $Z_{\dot{w}}$ for heave can be assumed to be the same as for sway, Eq. (10), because of symmetry in the torpedo-shaped hull. For the same reason, we use the same drag coefficient value, i.e., $C_{D_{heave}} = 1.2$.

2.5 Yaw Motion

External moments in the yaw rotational motion are moments due to the thrusters, hull drag, and added mass. The governing equation for yaw motion, Eq. (2), becomes (Helgason, 2012)

$$I_z\dot{r} = -D_{yaw}r + M_{yaw}, \quad (12)$$

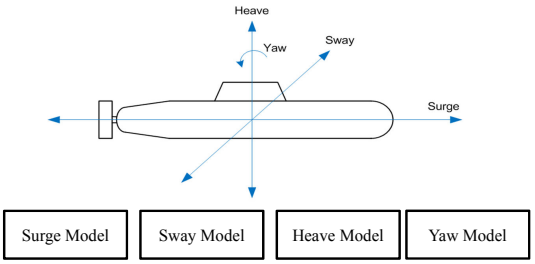

Figure 3: The four non interacting models of the simulator for each of the degrees of freedom.

where D_{yaw} is the hydrodynamic drag for yaw, and M_{yaw} is the yawing moment due to the thrusters. The drag is modelled using Eqs. (7) and (8). The quadratic drag coefficient is estimated based on experimental results for cylinder in cross-flow. We assume that each half of the cylinder is in cross-flow with the resulting force acting in it's center. Based on this the drag coefficient is found to by $C_{D_{yaw}} = 0.55$ (White, 2008).

3 SIMULATOR FRAMEWORK

The simulator was built in a plain block diagram environment using Simulink (Mathworks, 2011) where the differential equations for each degree of freedom (DOF) presented in Section 2 were implemented. The simulator structure is based on four non interacting models, each corresponding to a separate DOF (Fig. 3). Motion of the AUV along each DOF is simulated at a time and the combination of all the four models yields a simulation of the overall motion.

Due to length limitations, the models cannot be described in detail. However, the general structure of each model is shown in Fig. 4. The first block on the left is the input signal generator. In the second block, the thruster characteristics are defined. The main thruster at the rear is used for surge motion, while different thrusters are used for the other DOF's.

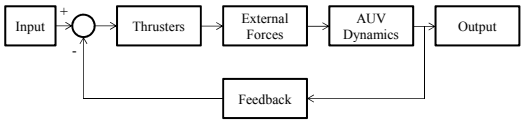

Figure 4: The basic block structure for each of the simulation models.

The third block represents the external forces acting on the AUV, such as drag, added mass, gravity, and buoyancy. The fourth block represents the AUV dynamics, which is different for each DOF, as described in Section 2. The block farthest to the right produces the simulation output, such as depth, heading

and position. The bottom block represents the feedback from the sensors (including any time delays). A detailed description of each model is given in (Helgason, 2012).

4 EXPERIMENTAL TESTING

In order to gather data for validating and tuning the simulator, several experiments were performed using the Gavia AUV. In this section, we describe the experimental approach and setup for open and closed loop testing.

4.1 Approach

The simulator can handle AUV motion in surge, sway, heave, and yaw. Therefore, data on the vehicle behaviour in all those directions is required for the simulator validation. Figure 5 shows where forces are needed for each direction. The testbed AUV only has a rear mounted propeller and can, therefore, only move in the surge direction. Additional thrusters were mounted on to the hull to achieve the desired motion. For each direction, both the open and closed loop performance were studied. In particular, we studied the response as a function of the thruster load, as well as different PID controller settings.

4.2 Setup

A pair of externally mounted thrusters were used for the experimental testing, aside the case of surge, where the rear mounted propeller was used. The thrusters were installed on a bracket which was mounted on the sides of the AUV hull as shown in Fig. 6. A plastic pipe was included in the bracket to provide buoyancy to balance the weight of the thruster. The thrusters are manufactured by Seabotix and are controlled by a Devantech MD22 motor controller. Figure 7 shows a thruster mounted on the bracket. Figure 8 shows the Gavia AUV with two thrusters mounted on it's side for sway testing. All tests were performed in an indoor swimming pool of 3 m depth.

5 MODEL VALIDATION AND TUNING

In this section, we present the results obtained in the experiments described in Section 4 and compare them with numerical results obtained by the model presented in Sections 2 and 3. In particular, we present

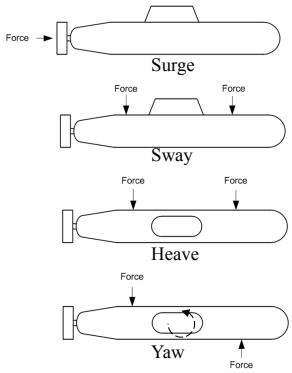

Figure 5: Experimental setup of the forces acting on the AUV hull for testing of each of the degree of freedom.

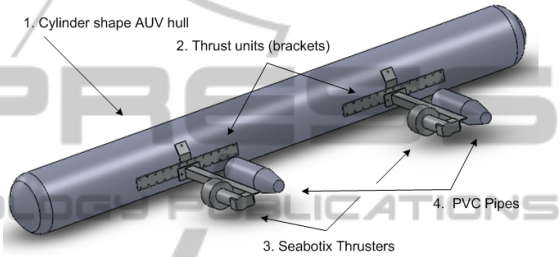

Figure 6: A sketch of the bracket and thrusters mounted on the hull of the AUV.

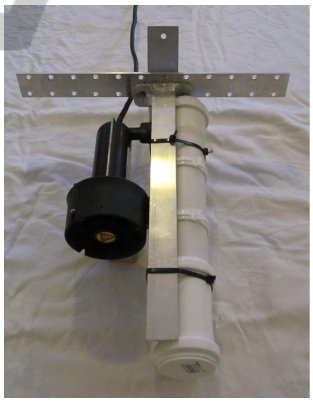

Figure 7: An assembly of the thruster, bracket and float.

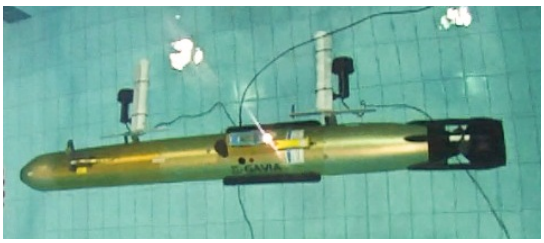

Figure 8: The Gavia AUV with the thruster assembly mounted on the sides during testing.

results for surge, sway, and yaw motions. The heave model is identical to the sway model.

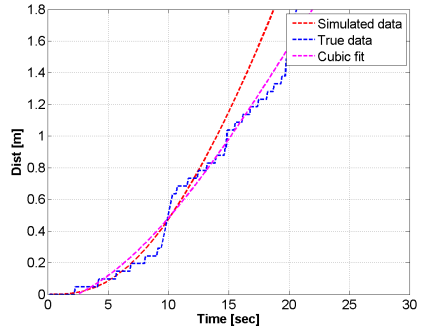

(a)

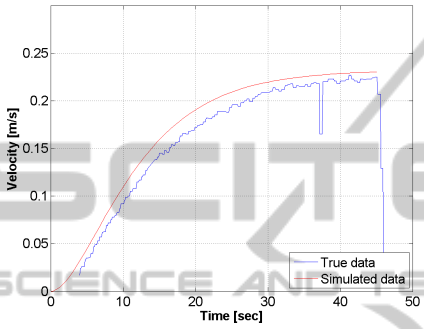

(b)

Figure 9: Surge open loop response for the propeller at 197 rpm (a) distance as a function of time, here the cubic fit is a polynomial fit to the true data used for comparison with the simulation, and (b) velocity as a function of time.

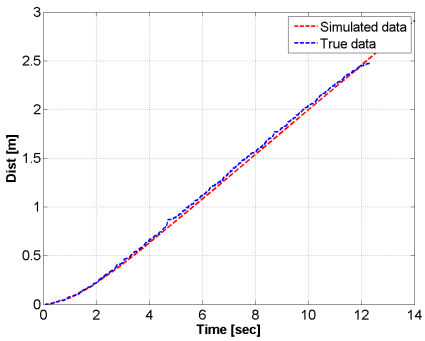

(a)

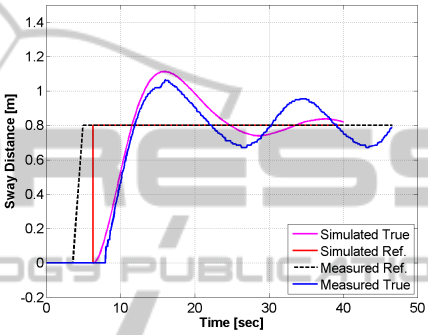

(b)

Figure 10: Sway responses (a) open loop with constant thrust of 0.5, and (b) closed loop with PID values of $P = 30$, $I = 0$, and $D = 0$.

5.1 Surge

Open loop response for surge forward motion are shown in Fig. 9 for the propeller at 197 rpm. A multiplicative tuning factor was applied to the model. The simulation model follows the experimental data for the first 12 seconds or so. The discontinuous shape of the experimental data is due to a low sampling rate of the sensors.

5.2 Sway

Open and closed loop sway responses are shown in Fig. 10. Here the quadratic drag term was tuned with a multiplicative constant to match the data in the open loop response. In the closed loop test, the AUV was translated by 80 cm.

The results show that the control system is able to quickly reach the translated distance, but overshoots by approximately 23 cm and converges towards the reference value slowly. The simulator follows the experimental results quite well, but overshoots by 30 cm, and converges more quickly towards the reference value. This indicates the discrepancy between the experimental and simulation configurations.

5.3 Yaw

Open and closed loop yaw responses are shown in Fig. 11. Here, as in the case of sway, the quadratic drag term was tuned with a multiplicative constant to match the data in the open loop response. In the closed loop test, the AUV was rotated by 40 degrees.

The results show that the control system quickly rotates the AUV towards the reference value, but overshoots by about 14 degrees. However, it recovers swiftly and reaches the reference value within 15 to 20 seconds. The simulation follows the data closely throughout the data series.

6 CONCLUSIONS

A simulation model for the motion of torpedo-shaped AUVs at low-speed was presented. The model is based the general equations of motion for marine vehicles. The hydrodynamic forces acting on the AUV hull were modelled using strip theory, experimental data, and computational fluid dynamics. The simulation model was implemented using a commercially available software and validated using experimental

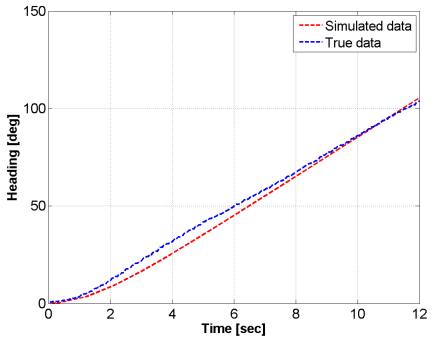

(a)

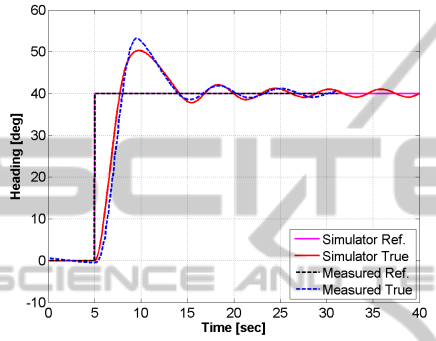

(b)

Figure 11: Yaw responses (a) open loop with constant thrust of 0.5, (b) closed loop with PID values of $P = 2$, $I = 0$, and $D = 0$.

data obtained from a commercially available AUV. The results show that the simulation model captures the AUV motion at low-speed and compares well with the experimental data.

The results of the research are promising and suggest that torpedo-shaped AUVs can be effectively controlled at low-speed with only a few thrusters. The next step in our work is to construct modules for the testbed AUV which contain thrusters within them. Incorporate these modules into the AUV and repeat the experimental testing. In the future, we will consider what type of thrusters are most suitable, i.e., the typical propeller thrusters, or more novel devices, such as vortex ring generators or pulsating membranes.

ACKNOWLEDGEMENTS

We would like to thank the University of Iceland for lending us their Gavia AUV to perform the experiments. We would also like to acknowledge the staff at Teledyne Gavia ehf. for their assistance during this work.

REFERENCES

Allen, B., Vorus, W., and Prestero, T. (2000). Propulsion system performance enhancements on remus auvs. In *OCEANS 2000 MTS/IEEE Conference and Exhibition*, volume 3, pages 1869–1873. IEEE.

Ananthakrishnan, P. and Decron, S. (2000). Dynamic stability of small and mini-autonomous underwater vehicles: Part i. analysis and simulation for mid water applications. Technical report, Technical Report, Florida Atlantic University, Florida.

Braunl, T., Boeing, A., Gonzalez, L., Koestler, A., and Nguyen, M. (2007). Design, modelling and simulation of an autonomous underwater vehicle. *International Journal of Vehicle Autonomous Systems, 4*, 2(3):106–121.

Clark, T., Klein, P., Lake, G., Lawrence-Simon, S., Moore, J., Rhea-Carver, B., Sotola, M., Wilson, S., Wolfskill, C., and Wu, A. (2009). Kraken: Kinematically roving autonomously kontrolled electro-nautic. *47th AIAA Aerospace Sciences Meeting Including the New Horizons Forum and Aerospace Exposition*, Orlando, Florida.

de Barros, E., Dantas, J., Pascoal, A., and de Sá, E. (2008). Investigation of normal force and moment coefficients for an auv at nonlinear angle of attack and sideslip range. *IEEE Journal of Oceanic Engineering*, 33(4):538–549.

Eastman, D., Lambrechts, P., and Turevskiy, A. (2009). Design and verification of motion control algorithms using simulation. *Embedded Systems Conference*, pages 1–4.

Fossen, T. (1994). *Guidance and Control of Ocean Vehicles*. John Wiley & Sons.

Helgason, B. (2012). Low speed modeling and simulation of gavia auv. Master's thesis, Reykjavik University.

Kennedy, J. (2002). Decoupled modelling and controller design for the hybrid autonomous underwater vehicles: Maco. Master's thesis, Univeristy of Victoria.

Mathworks (2011). *Simulink/Matlab*.

Wang, W. and Clark, C. (2007). Modeling and simulation of the Videoray Pro III underwater vehicle. *OCEANS 2006-Asia Pacific*, pages 1–7.

White, F. M. (2008). *Fluid Mechanics*. McGraw-Hill, 6 edition.